structural grounds ring fission probably occurs in solution, but the rate of ring closure is rapid, and the biradical returns to the starting material without any chemical consequence. Thus this material is a potential UV photostabilizer since it channels radiation energy efficiently to thermal energy without chemical change.[20]

In solid matrices little change is to be expected in the rate of ring fission since this is primarily dependent on the overlap between the chromophore (CO) and the acceptor cyclopropyl bond. Thus, irradiation should lead to the formation of the biradical at almost the same rate as in solution. For any process to compete with ring closure in the solid matrix it either should have an intrinsically lower activation energy or its activation energy must be lowered in the matrix owing to favorable conformations of the rigid molecules. The reaction involved here is 1,2 hydrogen migration. If this reaction had an intrinsically lower activation energy than ring closure, some migration product should have been observed at room temperature. The absence of such product formation in photolyses at room temperature could be explained if it is assumed that there is a much smaller Arrhenius factor for 1,2 hydrogen migration than for ring closure, which is not unreasonable to expect. The other possible explanation is that the molecules are frozen in conformations in the solid matrix that favor 1,2 hydrogen migration. Efficiency studies, stereochemical probes, and the temperature dependence of the rate of reaction should provide information regarding this possible rationalization for the difference in reactivity of **6** in solution and in solid matrices.

A point of spectroscopic importance concerns the observation of multiple phosphorescence from 2-spirocyclopropyl-1-indanone in several glass matrices. This molecule has no enolizable α hydrogen, which in this case eliminates Lim's proposal[12] of emission due to enol formation. Wagner and co-workers[13] reported dual phosphorescence from alkyl aromatic ketones, which was attributed to emission from $^3n,\pi^*$ excited states frozen in the ground-state conformation and from conformationally relaxed excited states. In evidence it was shown that the emission intensities of the various components are viscosity dependent. Similarily the phosphorescence of **6** in rigid glasses such as MCH, E/M, or PMMA at 77 K exhibited multiple emission, while in a less rigid glass (isopentane) it exhibited predominantly the low-energy part of the spectrum, in analogy with Wagner's observations.

Acknowledgment. We thank the National Research Council of Canada for support of part of this work and Professor P. J. Wagner for his valuable comments.

References and Notes

(1) D. G. Marsh and J. N. Pitts, Jr., *J. Am. Chem. Soc.*, **93**, 326 (1971), and references cited therein.
(2) H. E. Zimmerman and T. W. Flechtner, *J. Am. Chem. Soc.*, **92**, 6931 (1970), and references cited therein.
(3) J. K. Crandall and R. J. Seidewand, *J. Org. Chem.*, **35**, 697 (1970).
(4) D. R. Morton, E. Lee-Ruff, R. M. Southam, and N. J. Turro, *J. Am. Chem. Soc.*, **92**, 4349 (1970); N. J. Turro and D. R. Norton, *ibid.*, **93**, 2569 (1971); D. R. Norton and N. J. Turro, *ibid.*, **95**, 3947 (1973).
(5) Cf. also A. Sonoda, I. Moritani, J. Miki, and T. Tsugi, *Tetrahedron Lett.*, 3187 (1969); A. Sonoda, I. Moritani, J. Miki, T. Tsugi, and S. Nishida, *Bull. Chem. Soc. Jpn.*, **45**, 1777 (1972). These authors photolyzed **3** in hexane and obtained **4** together with a trace of 2-ethylcyclopentanone derived by cleavage of the cyclopropane ring.
(6) Cf. also N. J. Turro, W. E. Farneth, and A. Devaquet, *J. Am. Chem. Soc.*, **98**, 7425 (1976).
(7) It may be noted, however, that geminal dimethyl substitution on the cyclopropyl ring of **3** leads to photochemical cleavage of the cyclopropyl ring via an intermediate of type 1.[4]
(8) Compound **6** has previously been prepared by a different route: R. Fraisse-Jullien and C. Frejaville, *Bull. Soc. Chim. Fr.*, 219 (1970).
(9) K. Hoffmann and H. Schellenberg, *Helv. Chim. Acta*, **27**, 1782 (1944).
(10) M. Mühlstädt and H.-J. Gensrich, *J. Prakt. Chem.*, **34**, 139 (1966).
(11) G. P. Newsoroff and S. Sternell, *Aust. J. Chem.*, **25**, 1669 (1972).
(12) Y. Kanda, J. Stanislaus, and E. C. Lim, *J. Am. Chem. Soc.*, **91**, 5085 (1969).
(13) P. J. Wagner, M. May, and A. Haug, *Chem. Phys. Lett.*, **13**, 545 (1972).
(14) J. Kolc, *Tetrahedron Lett.*, 5321 (1972).
(15) H. Murai and K. Obi, *J. Phys. Chem.*, **79**, 2446 (1975), and references cited therein.
(16) N. J. Turro, V. Ramamurthy, W. Cherry, and W. Farneth, *Chem. Rev.*, **78**, 125 (1978).
(17) M. Berger and C. Steel, *J. Am. Chem. Soc.*, **97**, 4817 (1975).
(18) J. Kolc and J. Michl, *J. Am. Chem. Soc.*, **92**, 4147 (1970).
(19) J. Kolc and J. Michl, *J. Am. Chem. Soc.*, **95**, 7391 (1973).
(20) For a very recent study of the photolysis of alkyl-substituted spiro[*n*.2]-alkan-2-ones in solution, see E. Lee-Ruff and P. G. Khazanie, *Can. J. Chem.*, **56**, 803 (1978).

Carbanions, Electron Transfer vs. Proton Capture. 6. Determination of the Effect of Ion Pairing on the Electron-Transfer Equilibrium between Fluoradenide Ion and Nitrobenzene

Robert D. Guthrie* and Nam S. Cho

Contribution from the Department of Chemistry, University of Kentucky, Lexington, Kentucky 40506. *Received December 15, 1978*

Abstract: Fluoradenide ion in methanol reacts with nitrobenzene in an endoergic electron-transfer equilibrium which is followed by a rate-determining, second-order loss of nitrobenzenide ion. The rate constant for the second process has been determined by directly measuring the decay rate of photochemically produced nitrobenzenide using ESR spectrometry. Combination of K_a measurements with rate constants for loss of fluoradenide and loss of nitrobenzenide allows calculation of the effect of reaction variables on the electron-transfer equilibrium constant. This method has been used to show that ion pairing, which can be detected spectroscopically for the carbanion, stabilizes this carbanion more than nitrobenzenide ion, driving the equilibrium toward carbanion. A similar effect is observed for the proton-transfer equilibrium. The phenomenon is explained in terms of competition between ion pairing and hydrogen bonding as a mode of carbanion stabilization in this protic, polar solvent.

In previous work, we have studied the competition for 9-methoxyfluorenide ion between $PhNO_2$ and methanol as a function of counterion.[1] In an attempt to remove the kinetic complications inherent in this system of low steady-state carbanion concentrations, we decided to study a stable carbanion for which proton capture was not a factor in determining electron-transfer efficiency. We were fortunate to find that the fluoradenide ion, FD^-, not only gives an electron-transfer re-

0002-7863/79/1501-4698$01.00/0

Table I. Near UV-Visible Spectra of the FD^- [a] Salts of Various Cations in Methanol at 30 °C

cation[b]	λ_{max}, nm	ion pairing
Li	360, 375, 536	free ion
K	359, 374, 536	free ion
K-18-crown-6	361, 377, 520, 554	ion pair
K-cryptofix(2.2.2)[c]	356, 376, 525, 550	ion pair
Cs	360, 370, 518, 543	ion pair
Me_4N	361, 376, 516, 549	ion pair
Me_4N-18-crown-6	360, 376, 520, 553	ion pair
$(n\text{-Bu})_4N$	363, 376, 525, 553	ion pair
K in *t*-BuOH	357, 373, 520, 553	ion pair

[a] FDH concentrations were between 6×10^{-3} and 3×10^{-5} M. [b] The positions and relative intensities of the maxima were independent of base concentration between 0.05 and 1 M. In the case of the crown ether–potassium complex, mixed spectra were obtained when $[\text{crown ether}]_0$ was less than $[KOMe]_0$. There was a slight hint of a double maximum developing in potassium methoxide at [KOMe] = 2 M at 65 °C. [c] 4,7,13,16,21,24-Hexaoxa-1,10-diazabicyclo[8.8.8]-hexacosane.

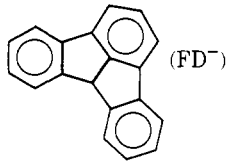

action with $PhNO_2$ in methanol but that changes in its visible spectrum can be associated with the onset of ion pairing.[2] Although preliminary investigation showed that a dramatic change in the rate of FD^- destruction could be associated with the conditions producing ion pairing, analysis of this effect in terms of individual rate constants was very speculative.[1,2] Further experimental work, centering on a careful ESR study of the reaction mixtures, now allows us to unequivocally determine the origin of these interesting counterion effects. These results are the subject of the present paper.

Because the important conclusions of this paper can be extracted from the data only through a rather involved calculation, we will attempt at this point to map our approach so that the reader can appreciate the necessity for the various experimental measurements which follow. Our goal will be to understand the factors which influence the rate of formation of products in the reaction of $PhNO_2$ and FD^- in methanol.

We will show that the simplest reaction sequence consistent with our data is that of Scheme I. It will be noted that, although we can follow the progress of the reaction by measuring $[FD^-]$ spectrophotometrically, the reaction conditions are such that FDH is not completely ionized. The establishment of equilibrium between FDH and FD^- is essentially instantaneous relative to the subsequent progress of the reaction so that k_H and k_h do not become independently involved in the rate expression. Nevertheless, because the overall reaction destroys an equilibrium mixture of FDH and FD^-, the rate of loss of this mixture, as followed by FD^- disappearance, will depend on the ratio of reactive species (FD^-) to unreactive species (FDH). Our first task will therefore be the collection of equilibrium data for this proton transfer under the conditions to be used in our kinetic study but with no electron acceptor present. Next, we will study the reaction of these equilibrium mixtures with $PhNO_2$ and establish the general characteristics of the kinetics and stoichiometry. We will then examine $[PhNO_2^-\cdot]$ during the reaction using ESR, demonstrating that it is an intermediate and, by measuring its maximum value, $[PhNO_2^-\cdot]_{max}$, provide necessary data for relating the rate constants for its formation to that for its destruction. It will also be necessary to justify our assumption that FD· can return to FD^-, i.e., that the electron transfer is reversible. This will be

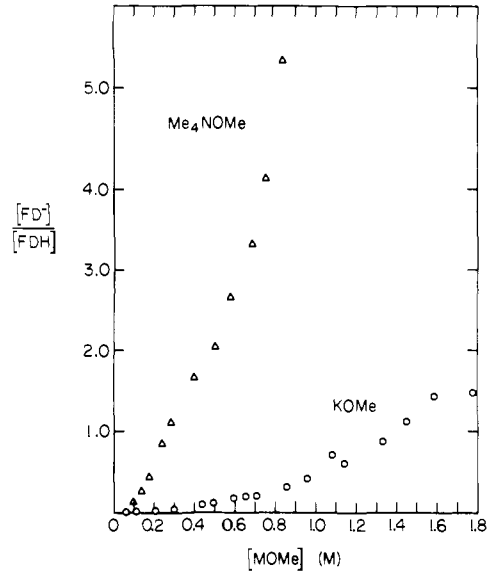

Figure 1. Dependence of FDH ionization on nature of counterion.

Scheme I

$$FDH \underset{k_h}{\overset{k_H[MeO^-]}{\rightleftharpoons}} FD^- \underset{k_{-e}}{\overset{k_e[PhNO_2]}{\rightleftharpoons}} FD\cdot + PhNO_2^-\cdot$$

$$FD\cdot \xrightarrow{k_a} (FD)_2 \qquad PhNO_2^-\cdot \xrightarrow{k_b} \text{azoxybenzene}$$

done by carrying out the reaction of FDH with $PhNO_2$ in the presence of a second carbon acid. Our final experimental measurement will be the independent determination of k_b under conditions comparable to the previous measurements in the absence of FD^-. This will allow us to relate $[PhNO_2^-\cdot]_{max}$ and the rate constant for loss of $[FD^-]$, k_{loss}, to k_e, k_{-e}, and k_a.

After collection of the experimental data as described, we will carry out a detailed analysis of Scheme I and derive the rate equations necessary to calculate $k_e\sqrt{k_a}/k_{-e}$. On the assumption that k_a is unaffected by changes in [MOMe] and by changes in M (K vs. Me_4N), we will assess the effect of these reaction variables on the electron-transfer equilibrium constant.

Results and Discussion

FD^- in Methanol. Fluoradene (FDH) reacts rapidly with alkali metal and tetraalkylammonium methoxide in methanol to establish an equilibrium with its red-colored conjugate base (FD^-). We have previously reported[2] that this anion can exist either as the "free ion" with a single absorption maximum in the visible region or as an ion pair which exhibits a double maximum. Since our preliminary communication, we have investigated several new cations and this data is summarized in Table I.

It is of particular interest to note that Cs^+FD^- is ion paired in methanol. Apparently a similar phenomenon to that which distinguishes the Cs^+ and K^+ salts of fluorene in THF[3] is also operative for Cs^+FD^- and K^+FD^- in methanol. Additional evidence that the spectral phenomena reported above are due to ion pairing is found in the apparent change in equilibrium constant for the reaction $FDH + MeO^- \rightleftharpoons FD^- + MeOH$ with changes in cation. A careful study of $[FD^-]/[FDH]$ as a function of [KOMe] and $[Me_4NOMe]$ is displayed in Table II and plotted in Figure 1. It was necessary to assume that the molar extinction coefficient, ϵ_{max}, of FD^- is the same for free ions and ion pairs. This could produce a small systematic error; however, the similarity of ϵ_{max} in Me_2SO-MeOH (4750) and that determined for FD^-Cs^+ in cyclohexylamine[4] (4200) in-

Table II. Effect of Cation Nature and Concentration on the Equilibrium FDH + $MeO^- \rightleftharpoons FD^-$ + MeOH at 30 °C in MeOH

[KOMe], M	$[FD^-]/[FDH]^a$	[Me_4NOMe], M	$[FD^-]/[FDH]^a$
		0.0516	0.034
0.057	0.0043		
		0.0963	0.121
		0.0982	0.134
0.111	0.0116		
		0.137	0.262
		0.174	0.434
0.206	0.0260		
		0.237	0.839
		0.279	1.106
0.292	0.0459		
		0.399	1.66
0.440	0.0945		
0.494	0.107		
		0.503	2.04
		0.579	2.65
0.593	0.175		
0.652	0.193		
		0.681	3.32
0.708	0.193		
		0.749	4.13
		0.831	5.33
0.856	0.311		
		0.934	10.9
0.956	0.422		
1.08	0.658		
1.14	0.603		
1.33	0.877		
1.45	1.12		
1.59	1.43		
1.77	1.45		
1.99	2.71		

[a] The concentrations of FDH used in this study ranged from 3×10^{-3} to 1×10^{-4} M. The extinction coefficient of FD^- was determined by adding Me_2SO to methoxide-methanol solutions. At 75% (v/v) Me_2SO, the value of ϵ was essentially steady at ϵ_{560} 4750. The previously reported value was ϵ_{556} 4200 in cyclohexylamine with cesium cyclohexylamide.[4] Other details are given in the Experimental Section.

dicates that no large differences in ϵ_{max} exist as a result of ion pairing.

It is clear from this data that not only does the apparent equilibrium constant ($[FD^-]/[FDH][MeO^-]$) change with $[MeO^-]$, a phenomenon noted for other carbanions in methanol,[4] but that the activity coefficients involved are also a function of counterion. Even at 0.05 M, which is the lowest [KOMe] at which measurement of $[FD^-]$ is practical, the value of $[FD^-]/[FDH]$ is nearly ten times greater with Me_4NOMe than with KOMe. The ratio of apparent equilibrium constants for the two cations remained a relatively constant factor of 20–25 between $[MeO^-]$ = 0.1 and 1.0 M, despite a roughly sevenfold change in both equilibrium constants.

It should be noted that a previous paper[1] in which we referred to our preliminary data for the FD^- system stated that the apparent K_a for FDH is more sensitive to [KOMe] than to [Me_4OMe]. This is clearly not true and, if anything, the opposite is the case. Actually, considering the errors inherent in the high [Me_4NOMe] data the increase in $[FD^-]/[FDH][MeO^-]$ with $[MeO^-]$ is approximately the same for both counterions. The error in our earlier experiments is now believed to be due to inadequate purification of the argon used as a protective atmosphere.

Reaction of FD^- with $PhNO_2$. We next investigated the reactions of the above-described methanolic solutions of FD^- salts with $PhNO_2$. These reactions proceed at convenient rates and produce bifluoradene in quantitative yield. GC analysis for $PhNO_2$ and its reduction products show clearly that the overall stoichiometry is that of eq 1.

$$6FDH + 2PhNO_2 \longrightarrow 3(FD)_2 + Ph{-}N{=}\overset{\overset{O}{\uparrow}}{N}{-}Ph \quad (1)$$

The reaction is first order in $PhNO_2$ as shown by the data listed in Table III and, in the case of KOMe, is first order in $[FD^-]$ as shown by the linearity of $\ln (A_0/A_t)$ vs. time through 3 half-lives and the constancy of the slope of these plots (k_{loss}) with changes in $[FDH]_0$.

Although it is possible to measure an approximate k_{loss} for all of the cations in Table I, accuracy is limited by the extreme insolubility of bifluoradene in methanol which interfered with spectroscopic measurements. Consistent and reproducible data were nevertheless obtained for one of the free ion systems (KOMe) and one of the ion pairing systems (Me_4NOMe). The data for KOMe are listed in Table IV and plotted in Figure 2.

Table III. Dependence of k_{loss}[a] on $PhNO_2$ Concentration

$[PhNO_2]$, M	$k_{loss} \times 10^4$, s^{-1}	k_2[b] $\times 10^3$, $M^{-1}\ s^{-1}$
0.0192	1.49	7.8
0.0385	3.38	8.8
0.0769	5.3	6.9
0.115	9.9	8.6
0.192	13.9	7.2

[a] k_{loss} is the first-order rate constant for the change in absorbance at 536 nm. $[FDH]_0 = 5 \times 10^{-4}$ M and [KOMe] = 0.415 M. The reaction was run in methanol at 30 °C. [b] $k_2 = k_{loss}/[PhNO_2]$.

Table IV. Effect of [KOMe] on k_{loss}[a] with $[PhNO_2]$ = 0.0192 M

[KOMe], M	$[FHD]_0 \times 10^4$, M	$k_{loss} \times 10^2/[PhNO_2]$, $M^{-1}\ s^{-1}$
0.070	60.0	0.125[b]
0.070	3.0	0.125[b]
0.18	4.6	0.328
0.42	3.9	0.781
0.60	3.9	1.46
0.74	6.0	1.61[b]
0.75	0.30	1.72[b]
0.91	3.5	2.76
0.98	4.5	4.46[c]
1.21	3.5	5.15

[a] First-order rate constants for loss of FD^- were determined spectrophotometrically in methanol. [b] These runs were made at approximately 25 °C; all other entries were at 30.0 °C. [c] This run was made with $[PhNO_2]$ = 0.0316 M.

Table V. Effect of [Me_4NOMe] on Reaction of FD^- [a] with $PhNO_2$ at 30.0 °C

[MeNOMe], M	$[PhNO_2]$, M	$k_{initial} \times 10^3/[PhNO_2]$,[b] $M^{-1}\ s^{-1}$	$k_{final}/[PhNO_2]$,[c] $M^{-2}\ s^{-1}$
0.052	0.0479	0.8	
0.094	0.0453	0.91	>25
0.232	0.0466	>1.1	7.95
0.374	0.0472	>1.1	1.85
0.475	0.0322	>6.2	1.30

[a] [FDH] ranged from 2.4×10^{-4} to 6.4×10^{-3} M. [b] Obtained from slope of plot of $\ln (1/A)$ vs. time where A = absorbance. [c] Obtained from plot of $1/A$ vs. time. Slope $\times \epsilon = k_{final}$.

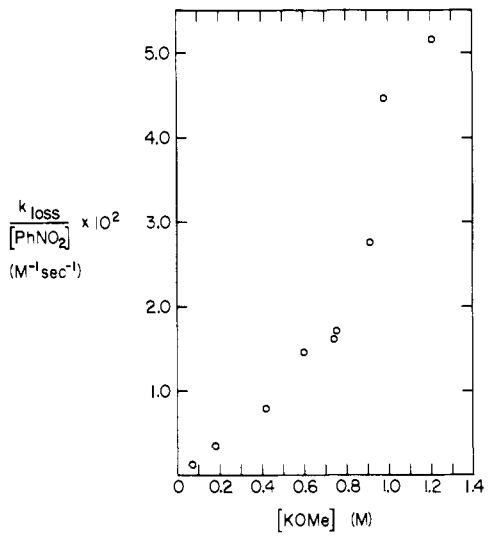

Figure 2. Effect of [KOMe] on k_{loss}.

Table VI. Dependence of $[PhNO_2^{-}\cdot]_{max}$ on [KOMe]

run	[KOMe], M	$[PhNO_2]$ $\times 10^2$, M	$[FDH]_0$ $\times 10^4$, M	$[PhNO_2^{-}\cdot]_{max}$ $\times 10^5$,[a] M	t_{max},[b] s
1	0.0101	36.1	5.17	1.34	800
2	0.0101	36.1	47.9	4.25	400
3	0.099	3.64	5.10	2.40	1800
4	0.099	3.64	4.44	2.27	2000
5	0.099	3.61	40.2	7.29	800
6	0.099	36.1	4.95	6.19	700
7	0.853	3.63	5.55	7.14	<230
8	0.853	3.63	5.09	6.96	194
9	0.849	0.378	4.67	2.23	900
10	1.27	0.378	4.67	2.55	500

[a] Determined by comparison to standard nitroxide solutions as described in the Experimental Section. [b] Approximate times at which $[PhNO_2^{-}\cdot]_{max} = [PhNO_2^{-}\cdot]$. The observed maxima were very broad and the uncertainty in t_{max} was at least 10% and in some cases as much as 50%. $T = 21 \pm 1$ °C.

Table VII. Dependence of $[PhNO_2^{-}\cdot]_{max}$ on [Me_4NOMe]

run	[Me_4NOMe], M	$[PhNO_4]$ $\times 10^2$, M	$[FDH]_0$ $\times 10^4$, M	$[PhNO_2^{-}\cdot]_{max}$ $\times 10^5$,[a] M	t_{max},[b] s
11	0.0106	36.1	5.31	1.33	780
12	0.0106	36.1	60.3	4.91	200
13	0.0513	35.9	5.29	4.19	900
14	0.0513	3.62	5.52	1.38	3 400
15	0.493	3.62	4.24	2.09	11 000

[a] See notes for Table VI. [b] See notes for Table VI.

The data for Me_4NOMe solutions differ from the KOMe data in several striking ways. At the lowest [Me_4NOMe] studied, 0.052 M, $k_{loss}/[PhNO_2]$ had an initial value of 8×10^{-4} M^{-1} s^{-1}, very similar to the corresponding value with KOMe. The first-order plot is linear through the first 30% of reaction but the slope proceeds to decrease thereafter until it is roughly 70% of its initial value during the third half-life. As the concentration of [Me_4NOMe] is increased, the initial rates seem to rise slightly, but the decrease of rate with time becomes more pronounced. At 0.23 M, the first-order plot shows distinct curvature, and after the first half-life the data gives a better fit to a second-order plot. By 0.48 M, second-order behavior is observed after the first 25% of reaction and the entire assembly of data points gives better linearity in a second-order plot. In Table V we present the different kinds of rate constants which can be estimated or determined for these runs. Figure 3 shows the data plotted as a first-order reaction and Figure 4 is a second-order plot of the same data.

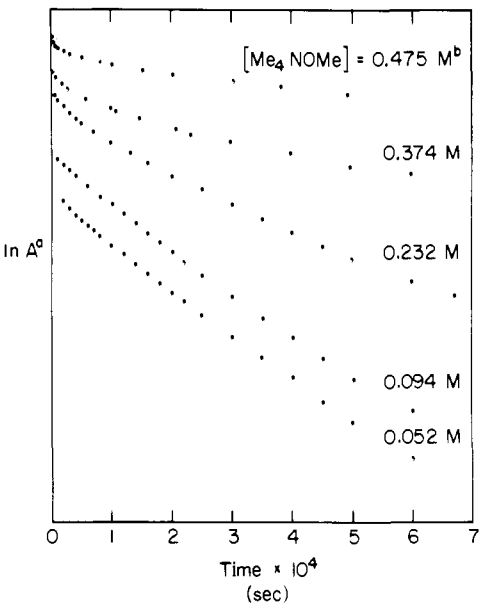

Figure 3. First-order plots for reaction of FD^- with $PhNO_2$ at different [Me_4NOMe]. (a) See note *a*, Table V. (b) See note *b*, Table V. The ln *A* axis has been displaced at different [MOMe] for clarity of presentation.

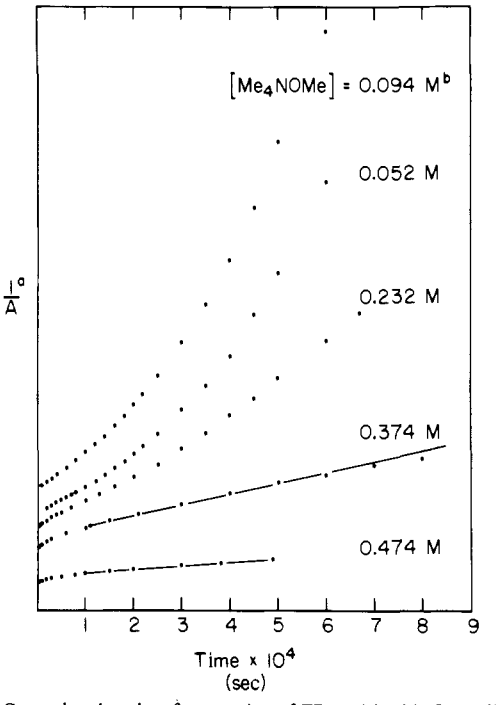

Figure 4. Second-order plots for reaction of FD^- with $PhNO_2$ at different [Me_4NOMe]. (a) See note *a*, Table V. (b) See note *c*, Table V. The $1/A$ axis has been displaced at different [MOMe] for clarity of presentation.

Analysis for $[PhNO_2^{-}\cdot]$ during the Reaction of FD^- with $PhNO_2$. By carrying out the reaction of FD^- with $PhNO_2$ in the cavity of an ESR spectrometer the intermediacy of nitrobenzenide ion ($PhNO_2^{-}\cdot$) can be demonstrated and its concentration can be measured. $[PhNO_2^{-}\cdot]$ increases to a maximum value, $[PhNO_2^{-}\cdot]_{max}$, and then decreases with time. $[PhNO_2^{-}\cdot]_{max}$ varies with $[FDH]_0$, $[PhNO_2]$, and [MOMe] as shown in Table VI for KOMe and Table VII for Me_4NOMe. As with the loss of FD^-, the data are similar at low [MOMe] but differ dramatically at high [MOMe]. At high

Table VIII. Effect of [MOMe] on k_b

M^+	[MOMe], M	$[PhNO_2] \times 10^2$, M	$3k_b$,[a] $M^{-1}\,s^{-1}$
K	0.0101	36.1	140.
K	0.099	36.1	14.2
K	0.099	3.64	17.4
K	0.858	3.65	38.2
			39.4
K	0.858	0.378	36.8
			48.0
Me_4N	0.0106	0.361	91.1
			102.4
Me_4N	0.0513	3.64	17.1
Me_4N	0.486	3.59	3.0

[a] See Experimental Section for details of calculations. The values of $3k_b$ are at 21 ± 1 °C. The factor of 3 results from the fact that $3PhNO_2^{-}\cdot$ are lost for every destruction event.

$[Me_4NOMe]$, the time of $[PhNO_2^{-}\cdot]_{max}$, t_{max}, increases to roughly 10^4 s whereas a decrease in t_{max} to 10^2 s is found at high [KOMe]. A higher value of $[PhNO_2^{-}\cdot]_{max}$ is also observed in the latter case.

Question of Reversibility of the Reaction of FD^- with $PhNO_2$. In order to carry out the kinetic analysis described in the following section, it is necessary to have information about the partitioning of FD· in Scheme I. In order words, we must know whether the electron-transfer process is reversible. In our previous study of 9-methoxyfluorenide with nitrobenzene,[1] it was concluded that the reaction was slightly reversible. Considering that the reactions following electron transfer should have similar rates in the two systems, it would reasonably be anticipated that electron transfer from FD^-, a more stable carbanion, should be even more reversible. To demonstrate this, we studied the reaction of FD^- with nitrobenzene in the presence of 9-aminofluorene as a second substrate. A 4.0×10^{-4} M methanolic solution of FDH in 0.301 M KOMe reacted with $PhNO_2$ (0.078 M) at a fourfold lower rate when 1.8×10^{-3} M 9-aminofluorene was included. As we had shown previously that 9-aminofluorene produces $PhNO_2^{-}\cdot$ in the presence of $PhNO_2$ and MeO^-[5], the observed rate reduction is assigned to an increase in the rate of conversion of FD· (fluoradenyl radical) to FD^- at higher $[PhNO_2^{-}\cdot]$. If the electron-transfer reaction were irreversible, changes in $[PhNO_2^{-}\cdot]$ would have no effect.[6]

An additional demonstration of reversibility is found in the behavior of $[PhNO_2^{-}\cdot]$ during the reaction. Our present techniques require a minimum time between mixing and measurement of 150 s. For some of the examples in Tables VI and VII this is sufficiently short to allow us to collect data during the time period when $[PhNO_2^{-}\cdot]$ is still increasing. Such measurements determine a minimum rate constant for the initial production of $PhNO_2^{-}\cdot$ and this was found to be significantly larger (in some cases by a factor of 10) than the rate constant for disappearance of $[FD^-]$ as determined later in the reaction. If the electron-transfer reaction were irreversible, initial and final rates would be equal.

Direct Determination of the Rate Constant for Destruction of $PhNO_2^{-}\cdot$, k_b. We were able to produce $PhNO_2^{-}\cdot$ in methanol–methoxide using the photochemical reaction reported by Ayscough and Sayent[7] and follow its decomposition by ESR. If $PhNO_2$ and MeOH–MeO^- are degassed and placed in a Pyrex tube in the cavity of an ESR spectrometer, no observable ESR signal is present after 30 min. If the tube is then removed and irradiated with visible light from a Hanovia medium-pressure lamp for 5 min (or even held under the overhead fluorescent lights) a substantial ESR signal appears. The spectrum is exclusively that of $PhNO_2^{-}\cdot$ and, in the darkness of the spectrometer cavity, decays in a cleanly second-order manner. The second-order rate constant is independent of $[PhNO_2]$ but is sensitive to [MOMe] in a significant way. The results of these measurements are presented in Table VIII.

At methoxide concentrations of 0.01 M the values of k_b are comparable for the two cations with the potassium case being slightly greater. As the base concentration is increased, k_b decreases for both cations and the decrease is almost exactly proportional to [MOMe]. As the [MOMe] concentration is raised above 0.1 M, however, k_b continues to decrease in the Me_4N^+ case but increases in the K^+ case. The result of these curious changes is that the decomposition of $[PhNO_2^{-}\cdot]$ is significantly faster in KOMe solutions at concentrations above 0.5 M. This then accounts for part of the cation dependence in k^*_{loss}.

Kinetic Analysis. Starting from Scheme I, it is possible to derive an equation relating k_{loss} to k_e, k_{-e}, k_a, and k_b as follows. Applying the steady-state approximation to [FD·] and $[PhNO_2^{-}\cdot]$ gives the equations

$$2k_a[FD\cdot]^2 = k_e[FD^-][PhNO_2] - k_{-e}[FD\cdot][PhNO_2^{-}\cdot] \quad (2)$$

$$3k_b[PhNO_2^{-}\cdot]^2 = k_e[FD^-][PhNO_2] - k_{-e}[FD\cdot][PhNO_2^{-}\cdot] \quad (3)$$

respectively. The stoichiometric factors used for k_a and k_b are those expected for the destruction of these two species but have no effect on our calculation, provided that they are used consistently. The kinetic order for destruction of nitrobenzenide is dependent on mechanism but we have shown that it is second order under the conditions of our experiments. (See preceding section.) Combination of eq 2 and 3 gives

$$[FD\cdot] = (3k_b/2k_a)^{1/2}[PhNO_2^{-}\cdot] \quad (4)$$

Rearrangement of eq 2 gives

$$[FD\cdot] = k_e[FD^-][PhNO_2]/(k_{-e}[PhNO_2^{-}\cdot] + 2k_a[FD\cdot]) \quad (5)$$

and substitution of the value of [FD·] from eq 4 into the denominator of eq 5 gives

$$[FD\cdot] = k_e[FD^-][PhNO_2]/([PhNO_2^{-}\cdot] \times (k_{-e} + (6k_ak_b)^{1/2})) \quad (6)$$

At this point we are prepared to substitute in the basic rate equation for loss of $[FD^-]$. Temporarily simplifying the situation by assuming that $[FD^-]/[FDH] \gg 1$ at equilibrium gives

$$-d[FD^-]/dt = k_e[FD^-][PhNO_2] - k_{-e}[FD\cdot][PhNO_2^{-}\cdot] \quad (7)$$

which, with substitution of [FD·] from eq 6, gives

$$-d[FD^-]/dt = [PhNO_2] \times [FD^-]k_e/((k_{-e}/(6k_ak_b)^{1/2}) + 1) \quad (8)$$

If electron transfer is reversible, $k_{-e} \gg \sqrt{6k_ak_b}$ and therefore the pseudo-first-order rate constant for loss of FD^- (obtained with excess $PhNO_2$) is given by

$$k^*_{loss} = k_e(6k_ak_b)^{1/2}[PhNO_2]/k_{-e} \quad (9)$$

As mentioned previously, the situation is complicated somewhat by the fact that FDH is not completely ionized and therefore the observed first-order rate constant, k_{loss}, is smaller than that expressed in eq 9, which assumes $FD^- \gg FDH$. Their relationship is given in the equation

$$k_{loss}([FDH] + [FD^-])/[FD^-] = k^*_{loss} \quad (10)$$

In principle, eq 9 and 10 accomplish our goal of enabling us to calculate $k_e\sqrt{k_a}/k_{-e}$. The determinations of ([FDH] +

Table IX. Calculation of k_{loss} from ESR Data in Tables VI, VII, and IX

run	M	[MOMe], M	$k_{loss} = [PhNO_2^{-}\cdot]^2 3k_b/([FDH] + [FD^-])$, s^{-1}	$k_{loss}/[PhNO_2]$, $M^{-1}\,s^{-1}$
1	K	0.0101	5.17×10^{-5}	1.43×10^{-4}
2	K	0.0101	5.43×10^{-5}	1.50×10^{-4}
3	K	0.099	1.91×10^{-5}	5.25×10^{-4}
4	K	0.099	1.98×10^{-5}	5.44×10^{-4}
5	K	0.099	2.16×10^{-5}	5.98×10^{-4}
6	K	0.099	1.53×10^{-4}	4.21×10^{-4}
7	K	0.853	4.40×10^{-4}	1.21×10^{-2}
8	K	0.853	4.63×10^{-4}	1.27×10^{-2}
9	K	0.849	4.83×10^{-5}	1.28×10^{-2}
11	Me_4N	0.0106	3.34×10^{-5}	9.25×10^{-5}
12	Me_4N	0.0106	3.92×10^{-5}	1.08×10^{-4}
13	Me_4N	0.0513	6.42×10^{-5}	1.79×10^{-4}
14	Me_4N	0.0513	6.12×10^{-6}	1.69×10^{-4}
15	Me_4N	0.493		

Table X. Calculation of $k_e\sqrt{k_a}/k_{-e}$

M	[MOMe], M	$[FD^-]^a/[FDH]$	$k^*_{loss}/PhNO_2\sqrt{3k_b} = k_e\sqrt{2k_a}/k_{-e}$
K	0.0101	$<0.001^b$	$>1.23 \times 10^{-2}$ [d]
K	0.099	0.010	1.33×10^{-2} [d]
K	0.85	0.320	8.4×10^{-3} [d]
Me_4N	0.0106	$0.001-0.007^c$	$10.1-1.5 \times 10^{-3}$ [d]
Me_4N	0.0513	0.035	1.25×10^{-3} [d,e]
Me_4N	0.493	2.1	9.0×10^{-5} [e]

[a] From data in Table II. [b] $[FD^-]$ cannot be measured under these conditions. It is assumed that $[FD^-]/[FDH]$ will be at least proportional to [KOMe]. [c] The upper value assumes proportionality to [Me_4OMe]. The lower is the value used for [KOMe] = 0.01 M. It may be safely assumed that both $[FD^-]/[FDH]$ and $k_e\sqrt{k_a}/k_{-e}$ will become cation independent at very low [MOMe]. [d] Calculated using ESR data only. [e] Calculated using ESR data and spectrophotometric data obtained during the last run of Table V.

$[FD^-])/[FD^-]$, k_{loss}, and k_b have all been described previously. Under some sets of conditions, however, it is not possible to use this method. This is true when the reaction does not follow pseudo-first-order kinetics, as is the case with [Me_4-NOMe] above 0.2 M, or when the $[FD^-]$ is too low to follow spectrophotometrically as with [KOMe] = 0.01 M. For these situations, an alternative calculation is available, based on ESR data obtained during the reaction. Equation 3 is used, but is invoked only at t_{max}. This is legitimate because, at the time when $[PhNO_2^{-}\cdot]$ reaches its maximum value, $d[PhNO_2^{-}\cdot]/dt = 0$ independent of whether this is a good approximation at other times during the reaction. Substitution of [FD·] from eq 4 into eq 3 leads to the equation

$$[PhNO_2^{-}\cdot]_{max}^2 = k_e[FD^-] \times [PhNO_2]/(3k_b(1 + (k_{-e}/(6k_ak_b)^{1/2}))) \quad (11)$$

and the reversibility assumption converts this to the equation

$$[PhNO_2^{-}\cdot]_{max}^2 = [FD^-][PhNO_2](k_e/k_{-e})(2k_a/3k_b)^{1/2} \quad (12)$$

Equation 12 can then be used to calculate $k_e\sqrt{k_a/k_b}$ provided that $[FD^-]$ is known at t_{max}. Because the required value of $[FD^-]$ was found to be rather close to $[FD^-]_0$, the method used for its estimation was not critical to the calculation. It was, of course, necessary to know the extent to which $[FDH]_0$ was converted to FD^- at the [MOMe] of each experiment and this presented a problem at low [MOMe].

Each of the two calculational techniques described above was used with that data in Tables VI–VIII to which it was applicable. Where both methods could be employed, agreement was very good. The exact method applied at each [MOMe] will be described in the next section.

An additional interesting feature of this treatment is that it allows k_{loss} to be calculated entirely from ESR data provided that the loss of substrate at t_{max} can be estimated. Combination of eq 9, 10, and 12 leads to the equation

$$k_{loss} = 3k_b[PhNO_2^{-}\cdot]_{max}^2/([FDH] + [FD^-]) \quad (13)$$

which gives k_{loss} without any time measurements provided that values of k_b are available. In the cases described in this study $[PhNO_2^{-}\cdot]_{max}$ occurs before much conversion to $(FD)_2$ has taken place. In such circumstances the equation

$$[FDH] + [FD^-] \simeq [FDH]_0 - [PhNO_2]_{max}^{-}\cdot \quad (14)$$

is a good approximation. If t_{max} is available, the accuracy of eq 14 can be checked using the value of k_{loss} calculated and a correction made in [FDH] + $[FD^-]$. In the calculations to be described, one iteration was sufficient.

Cation Dependence of the Electron-Transfer Equilibrium Constant, k_e/k_{-e}. To estimate the dependence of k_e/k_{-e} on M and [MOMe], we proceeded as follows. For all sets of conditions in Tables VI and VII, we solved eq 13 for k_{loss}. This was done using $[PhNO_2^{-}\cdot]_{max}$ (entries in Tables VI and VII), $3k_b$ from Table VIII, and $([FD^-] + [FDH])$ estimated at t_{max} by the procedure described at the end of the preceding section. The values of k_{loss} calculated in this fashion are based entirely on ESR data. (See Table IX.) Where comparisons can be made with spectrophotometric rate constants in Tables IV and V, the agreement is reasonably good. At 0.85 and 0.099 M KOMe, the ESR-derived rate constants are a factor of 2 lower than the values interpolated from Table IV, which is reasonable considering the roughly 9 °C lower reaction temperature for the former experiments. The value of $k_{loss}/[PhNO_2]$ listed in Table IX for 0.0513 M Me_4NOMe is low by a factor of 5 and this cannot be entirely explained on the basis of a difference in reaction temperature, but the uncertainty does not affect our conclusions.

With k_{loss} thus determined, we employed eq 10 to estimate k^*_{loss}, using Table II to obtain values of $[FDH]/[FD^-]$ at the [MOMe] desired. Equation 9 then gives $k_e\sqrt{2k_a}/k_{-e}$. An equivalent procedure avoids the calculation of k_{loss} by using eq 12 directly. The value of k_{loss} must still be estimated, however in order to determine $[FD^-]$ at t_{max}. The values of $k_e\sqrt{k_a}/k_e$ are listed in Table X.

The procedure described above is not applicable to runs carried out with [Me_4NOMe] > 0.2 M because the loss of FD^- is no longer first order. Equation 12 is still valid but a means to estimate $[FD^-]$ at t_{max} is required. In order to calculate $k_e\sqrt{k_a}/k_{-e}$ at [Me_4NOMe] = 0.48 we used the data in Tables VI and VII to estimate $[PhNO_2^{-}\cdot]_{max}$ and t_{max} under the conditions of the last entry in Table V. The measured value of $[FD^-]$ at t_{max} could then be used for calculation of $k_e\sqrt{k_a}/k_{-e}$. When this method was applied to data obtained at [Me_4NOMe] = 0.05 M, the value from the earlier described calculation was duplicated. All of this information is compiled in Table X.

It can be seen that contrary to our earlier analysis the electron-transfer equilibrium constant is essentially invariant with [KOMe], possibly decreasing slightly with increasing [KOMe]. With Me_4NOMe, there is a dramatic decrease in $k_e\sqrt{2k_a}/k_{-e}$ between [Me_4NOMe] = 0.05 M and 0.5 M. Even at 0.05 M, the value with Me_4NOMe is at least a factor of 10 below that for KOMe solutions of the same concentration. This difference is about the same as that between the values of $[FD^-]/[FDH][MeO^-]$ under the same conditions.

Table XI. Rate Constant Ratios for 9-Methoxyfluorenide Ion in Methanol at 30 °C

M^+	[MOMe], M	$k_D' \times 10^4$, $M^{-1}\ s^{-1}$	k_d/k_e	$k_{-e}/3\sqrt{k_a k_b}$[a]
Me_4N	0.056	0.76–0.85	4.6–5.3	0.45–0.68
	0.26	1.45	2.6	1.9
	0.64	2.93	0.71	10.4
K	0.20	0.74	2.8	0.79
	0.50	1.15	2.5	0.65
	1.07	2.34	1.3	1.08
	2.20	9.6	0.70	1.30

[a] Note that some calculational errors have been corrected in this column.

Conclusions

The results listed in the preceding sections allow us to draw the following conclusions about fluoradenide ion in methanol and its reaction with nitrobenzene.

1. The carbanion forms ion pairs with cations such as R_4N^+ and Cs^+. It also forms ion pairs with smaller alkali metals ions if they are complexed by crown ethers or cryptands. This is reflected in spectral changes (Table I) and in effective changes in K_a (Table II). Even in this polar protic medium, FDH is ionized to a 20-fold greater extent when KOMe is replaced by Me_4NOMe at high concentrations of MOMe.

2. The carbanion undergoes reversible electron transfer to $PhNO_2$ to form $PhNO_2^{-}\cdot$ which, in turn, is destroyed by second-order disproportionation.

3. The observed rate of the reaction of the carbanion with $PhNO_2$ is dramatically affected by the nature of the counterions present. With KOMe, the apparent first-order rate constant, k_{loss}, increases by a factor of ca. 30 for a ca. 15-fold increase in [KOMe]. With Me_4NOMe, the rate not only does not increase but actually changes kinetic order. The net result is a much less efficient oxidation of the carbanion–carbon acid mixture in the presence of Me_4NOMe in spite of the fact that more of the mixture is present as carbanion with this counterion.

4. We have been able to calculate values for $k_e\sqrt{k_a}/k_{-e}$ at various [MOMe]. Although we cannot calculate absolute values for the electron-transfer equilibrium constants from the available data, it is reasonable to assume that k_a has a value between 10^5 and $10^9\ M^{-1}\ s^{-1}$.[8] This means that $k_e/k_{-e} \simeq 10^{-6}$–$10^{-8}$. This is therefore an example of a reaction in which an endoergic electron-transfer process provides the main activation barrier.

5. Assuming that k_a, which represents a homolytic process, will be unaffected by [MOMe], the observed effects on $k_e\sqrt{k_a}/k_{-e}$ may be interpreted as changes in the electron-transfer equilibrium constant, k_e/k_{-e}. The data show that the stability of FD^- is increased relative to $PhNO_2^{-}\cdot$ by ion pairing with Me_4N^+. With KOMe, the stability of FD^- relative to MeO^- is increased with increasing [KOMe], but this has very little effect on the difference between FD^- and $PhNO_2^{-}\cdot$.

The stabilization of FD^- relative to MeO^- and $PhNO_2^{-}\cdot$ by ion pairing is viewed as a reflection of its highly delocalized character. The latter two ions and particularly MeO^- are stabilized by hydrogen bonding to a sufficient extent that the close approach of a cation would be endoergic. With FD^-, although hydrogen bonding to methanol may occur,[9] this would tend to localize charge. It is therefore energetically advantageous to replace such solvation by ion pairing provided that a large cation is available.

In addition to this study of fluoradenide ion, we have been able to use a photochemical reaction of nitrobenzene with methoxide–methanol, to produce nitrobenzenide ion. This allowed us to study the second-order decay of this species at various [MOMe] in methanol. At high concentrations we find a substantially lower second-order rate constant with Me_4NOMe than with KOMe. This factor also contributes to the inefficiency of the fluoradenide reaction when Me_4NOMe is present. When k_b is sufficiently small, $[FD^-]$ maintains a proportionality with $[PhNO_2^{-}\cdot]$ and the second-order nature of $PhNO_2^{-}\cdot$ loss is reflected in FD^- loss. The origin of the effect of M and [MOMe] on k_b is under investigation.

It seems appropriate to discuss the impact of this new data on the conclusions of our previous study of the reaction of 9-methoxyfluorenide ion with $PhNO_2$. The results of that study are given in Table XI. The rate constants are defined in ref 1 and have meanings analogous to those of the present paper. The designations k_d and k_D' refer to deuteron transfer to and from 9-methoxyfluorenide, respectively. Now that values of k_b are available, it can be seen that variations in k_b are responsible for part of the trend in $k_{-e}/3\sqrt{k_a k_b}$. Its invariance with [KOMe] reflects the behavior of $\sqrt{k_b}$ in the part of the concentration range where comparable data are available. For the Me_4NOMe case, the maximum variation of k_b taken from Table VIII for the concentration range of Table XI is a factor of 7. This means that k_{-e} increases by a factor of between 6 and 9 (assuming no variation in $\sqrt{k_a}$) over the tenfold range of increasing [Me_4NOMe]. Whether this reflects a decrease in k_e/k_{-e} or an increase in both k_e and k_{-e} cannot be determined from the available data. It is tempting to conclude that the stabilizing effect of Me_4N^+ on fluoradenide ion will be general for all carbanions. Studies that we will publish shortly show, however, that the magnitude of this effect with fluoradenide is rather unique even among carbanions of similar basicity. Methods which would allow further dissection of the ratios in Tables X and XI are under investigation. We will also apply the methods developed in this paper to other carbanions.

Experimental Section

Solvents and Solutions. The preparation of these has been described previously.[1,5] Nitrobenzene and 9-aminofluorene purifications have been described.[1,5] Fluoradene was prepared by the method of Baum and Schechter.[10] Solutions of fluoradene in methanol must be stored under argon and are likely to decompose slowly. The concentration of fluoradene must be checked by UV analysis at regular intervals.

Visible-UV Spectroscopic Measurements. A two-compartment mixing container was joined to a 1-cm quartz cell via a ground glass joint. For kinetic runs, nitrobenzene was placed in one of the compartments. The entire apparatus was connected to a vacuum system via an adapter section containing a 2-mm stopcock. The apparatus was evacuated and filled with argon that had been passed over a Chemalog R3-11 oxygen-removal catalyst. This argon purification was *absolutely critical* to the success of experiments with fluoradenide ion. Its solutions were not stable when commercial argon was used without purification. Solutions were degassed before transfer and introduced into the apparatus using a calibrated gas-tight syringe and degassed again by evacuation at −78 °C. The cell, mixing container, and adapter section, after filling with purified argon, was removed from the vacuum line, the solution allowed to equilibrate to the desired temperature, and mixing carried out. The quartz-cell portion of the apparatus was then placed in the thermostated cell compartment of a Cary 15 spectrophotometer.

ESR Measurements. Samples for measurements and kinetic runs were prepared exactly as described for the UV–visible studies above except that a 3-mm Pyrex tube served as the measurement cell. Measurements were carried out with a Varian E-109 Century Series ESR spectrometer with the 90° out-of-phase signal minimized. Concentrations were measured by comparing Hw^2 for the second peak to standard solutions of 4-acetamido-2,2′,6,6′-tetramethylpiperidino-1-oxyl (H = peak to peak amplitude, w = peak to peak width). Measurements for standard solutions were carried out in the same cell used for $PhNO_2^{-}\cdot$ studies and were proportional to concentration below 9×10^{-4} M. Reproducibility was within 10%. For the series of experiments described, the same cell was used for $[PhNO_2^{-}\cdot]_{max}$ measurements and for determination of k_b.

Irradiation Experiments. Irradiations were carried out by exposing the 3-mm tubular cell described above to light from a medium-pressure 450-W mercury lamp (Hanovia) with 0.1 M $FeCl_3$ solution as a filter. The tube was transferred to the cavity of an ESR spectrometer and the $PhNO_2^{-\cdot}$ peak described above was scanned at short intervals. A plot of $1/H \times w^2$ vs. time was linear. Its slope was proportional to $3k_b$ with the proportionality factor being determined by the above-described measurements on standard nitroxide solutions.

Acknowledgment. The authors express their gratitude to the National Science Foundation for a Grant, GP-42837-X, supporting this work.

References and Notes

(1) R. D. Guthrie, G. W. Pendygraft, and A. T. Young, *J. Am. Chem. Soc.*, **98**, 5877 (1976).
(2) R. D. Guthrie and N. S. Cho, *J. Am. Chem. Soc.*, **97**, 2280 (1975).
(3) J. Smid, *Angew. Chem., Int. Ed. Engl.*, **11**, 112 (1972).
(4) A. Streitwieser, Jr., D. G. Chang, and A. T. Young, *J. Am. Chem. Soc.*, **94**, 4888 (1972).
(5) R. D. Guthrie, D. P. Wesley, G. W. Pendygraft, and A. T. Young, *J. Am. Chem. Soc.*, **98**, 5870 (1976).
(6) A referee has pointed out that the observed rate reduction might be explained by a hydrogen-atom extraction from 9-aminofluorene by FD·. This seems to us an energetically unlikely reaction but we cannot rule out this alternative. The other indications of reversibility suggest that our interpretation of the 9-aminofluorene experiment is correct.
(7) P. B. Ayscough and P. P. Sayent, *Proc. Chem. Soc., London*, 94 (1963).
(8) (a) K. U. Ingold in "Free Radicals", J. K. Kochi, Ed., Wiley-Interscience, New York, 1973, p 52; (b) B. G. Gowenlock, P. P. Jones, and D. R. Snelling, *Can. J. Chem.*, **41**, 1911 (1963).
(9) T. E. Hogen-Esch, *J. Am. Chem. Soc.*, **95**, 639 (1973).
(10) (a) G. Baum in "Studies of Synthesis of Benzocyclopropenes. I. Thermolysis and Photolysis of Indazoles. II. Aryne Cyclization Processes", Ph.D. Dissertation, Ohio State University, 1965; (b) G. Baum, R. Bernard, and H. Shechter, *J. Am. Chem. Soc.*, **89**, 5307 (1967); (c) G. Baum and H. Shechter, *J. Org. Chem.*, **41**, 2120 (1976).

Generation of Butatrienone (Vinylideneketene) by Flash Vacuum Pyrolysis and Measurement of Its Microwave Spectrum

Ronald D. Brown,* Roger F. C. Brown, Frank W. Eastwood, Peter D. Godfrey, and Donald McNaughton

Contribution from the Department of Chemistry, Monash University, Clayton, Victoria, 3168, Australia. *Received January 2, 1979*

Abstract: Butatrienone (vinylideneketene) has been generated by flash vacuum pyrolysis of buta-2,3-dienoic trifluoroacetic anhydride. The microwave spectrum has been observed and assigned in the region 8–83 GHz. Rotational and centrifugal distortion constants have been determined for $CH_2{=}C{=}C{=}C{=}O$, $CHD{=}C{=}C{=}C{=}O$, and $CD_2{=}C{=}C{=}C{=}O$. The dipole moment was found to be $\mu_a = 1.967 \pm 0.019$ D ($6.47 \pm 0.06 \times 10^{-30}$ C·m). There is evidence that butatrienone is a planar molecule of C_{2v} symmetry, and that the heavy atoms lie along a straight line.

The generation of propadienone (methyleneketene) and the assignment of its microwave spectrum have recently been reported.[1-3] This provided a strong stimulus to attempting the synthesis and the study of the microwave spectrum of the next member, butatrienone (vinylideneketene), of the series formaldehyde, ketene, propadienone. Moreover, the rotational spectrum of propadienone implied some rather unsuspected properties of the molecule—either the chain of heavy atoms is nonlinear or there are unusually large vibrational effects upon the spectrum. It was of interest to determine whether these effects are further enhanced in the next member of the series. We report here the generation for the first time of butatrienone, and the assignment of the microwave spectra of butatrienone, monodeuterated butatrienone, and dideuterated butatrienone. The method of generation of butatrienone, a transient species, by pyrolysis of butadienoic trifluoroacetic anhydride is unsuitable for most experiments on chemical trapping or low-temperature collection, and further spectroscopic and chemical characterization will require an alternative method for its formation.

Experimental Section

Materials. Butadienoic acid, mp 65–66 °C (^{1}H NMR ($CDCl_3$) δ 5.29 ($CH_2{=}$), 5.68 (=CH–) (AB_2 system, J = 4.36 Hz), 10.2 (CO_2H)) was prepared from but-3-ynoic acid[4] by the method of Eglinton et al.[5]

[4,4-D_2]Butadienoic Acid. Treatment of but-3-ynoic acid (4.25 g) under the conditions described,[5] but using D_2O (100 mL, 99% isotopic purity), gave [4,4-D_2]butadienoic acid (1.8 g, 42% (^{1}H NMR ($CDCl_3$) δ 5.68 (s, =CH–), 10.5 (s, CO_2H)) probably partially deuterated in the 2 position. Mass spectral analysis of the pyrolysate of the resulting butadienoic trifluoroacetic anhydride (see below) showed a peak at m/e 68 attributed to $C_4D_2O^{+\cdot}$, while the monodeuterated species was undetectable. Repetition of the procedure using D_2O of 75 and 50% isotopic purity gave samples of butadienoic acid which on conversion to the mixed anhydride and pyrolysis showed peaks at m/e 68, 67, and 66 for the same ion corresponding to isotopic ratios D_2:DH:H_2 of 58:32:10 and 13:47:40, respectively, in the mass spectrometer.

Butadienoic Trifluoroacetic Anhydride (1). The mixed anhydride was prepared by a procedure similar to that of Emmons et al.[6] A solution of butadienoic acid (840 mg) in methylene chloride (1 mL) was cooled to 0 °C and trifluoroacetic anhydride (3 mL) was added. After 10 min the more volatile material was evaporated under partial vacuum and the residue was distilled from bulb to bulb (50 °C air bath, 20 mmHg) to yield the anhydride (1.4 g, 77%) as a colorless liquid: IR (neat) 1971, 1848, 1786 cm^{-1}; ^{1}H NMR ($CDCl_3$) δ 5.49 (CH_2), 5.81 (CH) (AB_2 system, J = 4.02 Hz); mass spectrum m/e 181 (M^+ + 1, 10%), 180.0037 ($M^{+\cdot}$, 22%, $C_6H_3O_3F_3$ requires 180.0034), 152 (22%), 97 (24%), 84 (14%), 69 (100%), 67 (76%), 66 (30%).

1,2,3-Butatrien-1-one (2). This was generated by flash vacuum pyrolysis of butadienoic trifluoroacetic anhydride (**1**).

$$CH_2{=}C{=}CHCO_2COCF_3\ (\mathbf{1}) \xrightarrow[\text{pyrolysis}]{\text{flash vacuum}} CH_2{=}C{=}C{=}C{=}O\ (\mathbf{2}) + CF_3CO_2H$$

The pyrolysis furnace was a 400 × 25 mm i.d. silica tube, heated to 520 °C. Spectra were obtained by pumping the pyrolysate directly through the spectrometer from the furnace. Spectra of the following compounds and mixtures were run separately at a pyrolysis temper-

0002-7863/79/1501-4705$01.00/0